Controlled Oxidation Level of Reduced Graphene Oxides and Its Effect on Thermoelectric Properties

Jaeyoo Choi[1], Nguyen D. K. Tu[1,2], Sang-Soo Lee[1,3], Hyunjung Lee[4], Jin Sang Kim[5], and Heesuk Kim*[,1,2]

[1]*Photo-electronic Hybrids Research Center, Korea Institute of Science and Technology (KIST), Seoul 136-791, Korea*
[2]*University of Science and Technology (UST), Daejeon 305-333, Korea*
[3]*KU-KIST Graduate School of Converging Science and Technology, Korea University, Seoul 136-701, Korea*
[4]*School of Advanced Materials and Engineering, Kookmin University, Seoul 136-702, Korea*
[5]*Electronic Materials Research Center, Korea Institute of Science and Technology (KIST), Seoul 136-791, Korea*

Abstract: We investigated the thermoelectric properties of reduced graphene oxide (rGO) as a function of the oxidation level of rGO. rGO among graphene derivatives was selected as a thermoelectric material since rGO bucky paper shows low thermal conductivity due to the phonon scattering at the junctions of rGO nanoplatelets. The oxdation level of rGO was controlled by differing the amount of chemical reductant (hydrazine) used to reduce graphene oxide (GO) to rGO, which correspondingly affected the electrical conductivity and Seebeck coefficient of rGO film. In this study, the maximum of figure of merit (ZT) was found to reach to 1.1×10^{-4} at 298 K for rGO reduced with the hydrazine of 1000 µL. These results provide the first experimental evidence that the thermoelectric performance of graphene and its derivative can be controlled by the oxidation level of graphitic nanoplatelets.

Keywords: reduced graphene oxide, oxidation level, thermoelectric properties.

Introduction

Recently, there has been of great interest in reducing the demand for fossil fuels by developing alternative renewable energy technologies. Especially, thermoelectric systems have emerged as a promising technique in harvesting electricity from waste heat or heat sources without moving mechanical components or hazardous working fluids.[1,2] The performance of thermoelectric materials is quantified by a figure of merit (ZT), given by

$$ZT = (S^2\sigma)T/\kappa \qquad (1)$$

where S, σ, T, and κ are the Seebeck coefficient, electrical conductivity, absolute temperature, and thermal conductivity, respectively. To get a high ZT value, high S, high σ, and low κ are required. In general, semiconductors are the best materials to achieve a good thermoelectric efficiency. However, typical thermoelectric semiconductor materials including bismuth telluride are expensive, chemically unstable and relatively difficult to process, yielding the limited use for thermoelectric devices.[3,4]

More recently, the thermoelectric property of graphene and its derivatives became a rising research topic because of the promising performances and tailorability. Previous theoreti-

cal works on the thermoelectric property of graphene demonstrated that the calculated ZT could be as high as 4 with Seebeck coefficient of more than 500 µV/K.[5,6] However, single or few layers graphene from chemical vapor deposition (CVD) or mechanical exfoliation only showed low Seebeck coefficient in the range of 30-80 µV/K at room temperature.[7,8] In addition, these graphenes showed no experimental ZT values due to their high thermal conductivities. Therefore, the investigation into thermoelectric properties of graphenes prepared by various methods such as chemical reduction of graphene oxides may facilitate to improve the thermoelectric performance and understand the intrinsic thermoelectric properties of graphenes.

In this study, we have selected reduced graphene oxide (rGO) as a thermoelectric material since rGO bucky paper shows low thermal conductivity due to the phonon scattering at the junctions of rGO nanoplatelets. In order to tune Seebeck coefficient and electrical conductivity of rGO, we systematically controlled the oxidation level of rGO and then investigated the correlation between the oxidation level and thermoelectric properties of rGO.

Experimental

Materials. Expandable graphite (natural grade, ~100 mesh, 99.9% with metals basis) was purchased from Asbury Graphite Mills and used as received. 98% H_2SO_4, 28% NH_3 aqueous

*Corresponding Author. E-mail: heesukkim@kist.re.kr

solution and 35% NH$_2$NH$_2$ aqueous solution with reagent grade were purchased from Sigma-Aldrich. KMnO$_4$ and 30% H$_2$O$_2$ aqueous solution were obtained from Yakuri. All the chemicals were used without further purification.

Preparation of Graphene Oxide (GO) and Reduced Graphene Oxide (rGO). GO was prepared by the modified Hummers method using expandable graphite flake as a starting material.[9,10] rGO was prepared *via* chemical reduction of GO by hydrazine. 250 mL of distilled water and 700 μL of 28% NH$_3$ aqueous solution were added to 100 mL of GO dispersion. Various amounts of 35 wt% hydrazine solution (30, 40, 75, 100, and 1000 μL) were added into each GO dispersion to control the oxidation level of rGO. Each mixture was stirred for 1 h at 95 °C and purified by dialysis for one week. For characterization of GO and rGO, their bucky papers by vacuum-filtration were dried at room temperature for 6 h, followed by heating at 95 °C for 1 day.

Characterization. GO and rGO were characterized by X-ray photoelectron spectroscopy (XPS, PHI 5800 ESCA System) using a monochromatized AlK$_\alpha$ source (*h*=1486.6 eV), a 90° angle between excitation and detection, and a 45° take-off angle. The source power was 10 kV×27 mA, and the analysis spot size was 400 μm^2. Spectra were analyzed using Voigt line-shapes, and a reduced χ^2 statistical analysis was used to characterize the quality of fit. Electrical conductivity measurements were performed using a four-point probe system consisting of a four-point cylindrical probe head (JANDEL Engineering), a direct current precision power source (Model 6220, Keithley), and a nanovoltmeter (Mode 2182A, Keithley). Seebeck coefficients of all rGO films were measured by Seepel instrument (Model TEP 600) at room temperature. The sample size for thermoelectric measurement was 2 cm× 2 cm and sample's thickness was approximately 100 μm. When we applied the temperature differences (0.5, 1.5, and 2.5 °C in one direction, and -0.5, -1.5, and -2.5 °C in the opposite direction) to the two ends of the sample, the probes measured the potential difference and calculated the Seebeck coefficients. We should also consider the linear correlation for the reliability of the measurement. The in-plane thermal conductivity of the rGO sample was obtained from the thermal diffusivity measured by laser flash system (LFA 457 NanoFlash, Netzsch), the specific heat measured by DSC (DSC7, Perkin-Elmer) and the density of the sample.

Results and Discussions

Control of the Oxidation Level of rGO. The oxidation level of rGO was controlled by the amount of chemical reductant, hydrazine, used to reduce GO to rGO (Figure 1(a)). During chemical reduction, many sp^3 carbon atoms bound to oxygen are recovered to sp^2 carbon atoms of graphene. Figure 1(b) shows the surface morphology of rGO bucky paper, demonstrating that rGO nanoplatelets are contacted with each other and rGO bucky film is uniform.
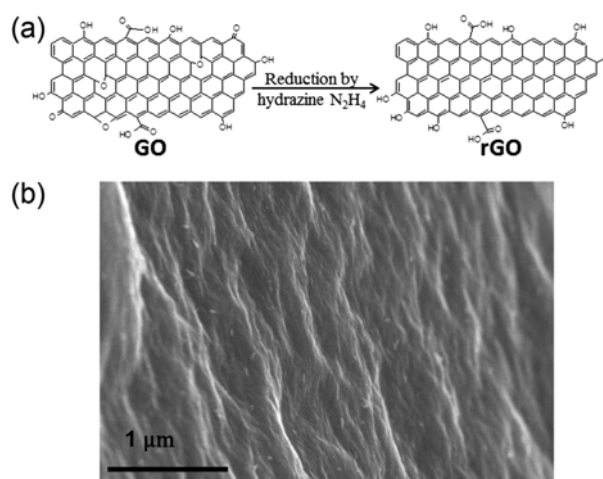

Figure 1. (a) Schematic illustration for the chemical reduction of GO to rGO, and (b) SEM image of rGO bucky paper prepared by vacuum filtration.

The oxidation level of rGO was quantitatively and qualitatively characterized by XPS. Figure 2(a) and (b) show high-resolution XPS spectra of the C(1s) and O(1s) regions before and after chemical reduction of GO with various amounts of hydrazine (GO and rGOs treated with 30 and 1000 μL hydrazine, respectively). Before chemical reduction, as-prepared GO is characterized by a C(1s) peak at 284.6 eV, with distinct two peaks at 286.7 and 288.2 eV. The peak at 284.6 eV arises from the non-oxygenated ring C (C-C bonds), whereas two peaks at 286.7 and 288.2 eV arise from the C in C-O bonds of hydroxyl and 1,2-epoxide functionalities and the carbonyl C in C=O bonds of carboxyl and ketone functionalities, respectively. After chemical reduction, the intensities of C(1s) peaks at 286.7 and 288.2 eV are much smaller than those of GO. These observations are consistent with the previous reports.[11-13] In addition, as the amount of hydrazine increases the peak intensities at 286.7 and 288.2 eV decrease, indicating that GO is more reduced with more hydrazine. The O(1s) peak of rGO also decreases as the amount of hydrazine increases. For quantitative characterization, the O/C area ratios of each sample, $A_{O(1s)}/A_{C(1s)}$, were calculated from the XPS data (Figure 2(c)). While the $A_{O(1s)}/A_{C(1s)}$ of GO is 1.24, those of rGO decrease from 0.85 to 0.32 as the amount of hydrazine increase from 30 to 1000 μL. It demonstrates that the oxidation level of rGO is controlled by the amount of hydrazine.

Thermoelectric Properties of rGO. Oxidized graphene has been generally known to exhibit very low electrical conductivity through formation of sp^3 carbon atoms bound to oxygen as well as structural defects.[13] Therefore, the chemical or thermal reduction of GO to rGO, *i.e.* restoration of sp^2 clusters would impart notable improvement of electrical conductivity to graphitic nanoplatelets. As shown in Figure 3(a), the electrical conductivity was dramatically changed in terms of the oxidation level ($A_{O(1s)}/A_{C(1s)}$) of rGO. While the electrical
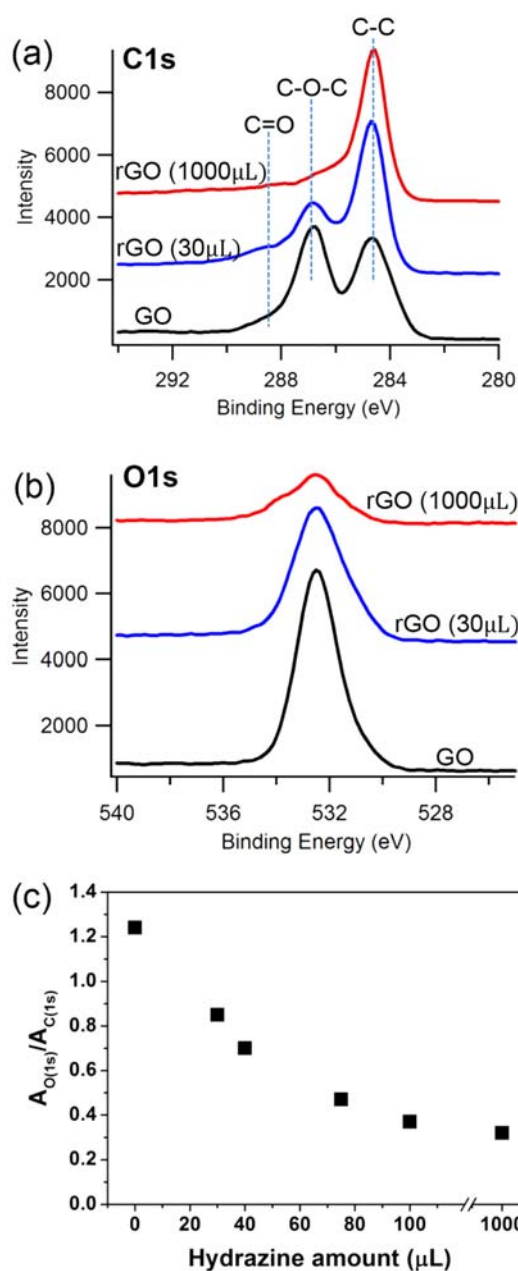
Figure 2. (a), (b) High resolution XPS spectra of the C(1s) and O(1s) regions before and after chemical reduction of GO with hydrazine (GO and two rGOs treated with 30 and 1000 μL hydrazine), and (c) O/C area ratios of rGO ($A_{O(1s)}/A_{C(1s)}$) as a function of hydrazine amount (μL).

conductivity of only about 0.14 S/m was obtained for rGO with the oxidation level of 0.85, the electrical conductivity was exponentially enhanced to near 880 S/m when the oxidation level was 0.32. On the other hand, as the electrical conductivity of rGO film increases from 0.14 to 880 S/m, the Seebeck coefficient of rGO decreases from 60 to 11 μV/K at room temperature. This trend is general in typical bulk semiconductors.[14] Insulators and semiconductors have large

Seebeck coefficients due to their low carrier concentration. However, low carrier concentration results in low electrical conductivity. Therefore, the increasing the electrical conductivity results in a decrease in the Seebeck coefficient. To deeply understand the correlation between the reduction level and the amount of carrier concentration, we measured the carrier concentration and mobility of rGO samples by Hall measurement. While the rGO sample with the electrical conductivity of 1.4 S/m shows the carrier concentration of 1.99×10^{16} cm^{-3} and the carrier mobility of 2.56 cm^2/V·s, the rGO with 654 S/m shows higher carrier concentration (6.01×10^{17} cm^{-3}) and mobility (1.88×10^2 cm^2/V·s). It could be due to more reduction of GO to rGO, *i.e.* more restoration of sp^2 clusters. Therefore, the reduction of GO to rGO, restoration of sp^2 clusters, leads to the increase of the carrier concentration, thereby increasing the electrical conductivity and decreasing the Seebeck coefficient. The maximum Seebeck coefficient of rGO (60 μV/K) is similar to those of single or few layers graphenes from CVD method or mechanical exfoliation.[7,8]

We can expect that further increase of hydrazine amount, *i.e.* lower oxidation level would correspond to electrical conductivity comparable to that of pristine graphite. However, as mentioned above, large electrical conductivity results in drop of Seebeck coefficient, which suppresses increase of ZT by
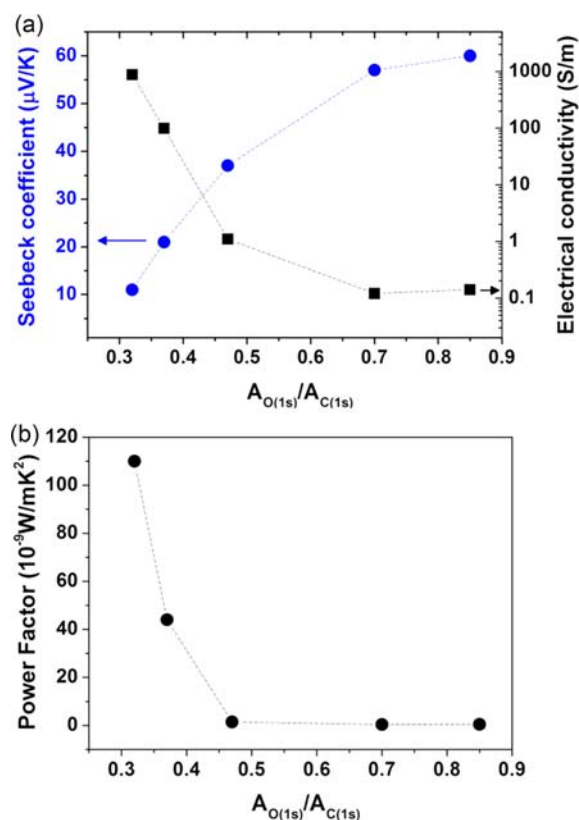

Figure 3. (a) Seebeck coefficients and electrical conductivities, and (b) power factors of rGO bucky papers as a function of O/C area ratios ($A_{O(1s)}/A_{C(1s)}$).

eq. (1). Therefore, it should be required to find optimum oxidation level of rGO for higher ZT rather than to seek perfect restoration of sp^2 clusters. Power factor is a powerful parameter to find the optimum oxidation level of rGO. Power factor ($S^2\sigma$) can be obtained from multiplication of electrical conductivity by square of Seebeck coefficient. As shown in Figure 3(b), the power factor is inversely proportional to the oxidation level just like the electrical conductivity. It is because Seebeck coefficient shows the small increase from 11 to 60 μV/K depending on the oxidation level of rGO while the electrical conductivity shows the large decrease with 3 orders of magnitude from 880 to 0.14 S/m. It corresponds to the trend of thermoelectric polymers reported previously.[15-20] In our study, the highest power factor (1.1×10^{-7} W/mK^2) was obtained from the electrical conductivity of 880 S/m and Seebeck coefficient of 11 μV/K at the oxidation level of 0.32.

The thermal conductivity of rGO film with the oxidation level of 0.32 (reduced with hydrazine of 1000 μL) was measured to 0.30 W/mK, which is 4 orders of magnitude lower than that of single-layer graphene (~5300 W/mK) due to the phonon scattering at the junctions of rGO nanoplatelets.[21] The maximum ZT of rGO was calculated to 1.1×10^{-4} from the thermal conductivity of 0.30 W/mK and power factor of 1.1×10^{-7} W/mK^2. rGO film shows a quite low ZT despite its low thermal conductivity, compared with the theoreticaly predicted thermoelectric properties of graphene.[5,6] A few previous theoretical researches report the optimum band gap of a typical inorganic thermoelectric semiconductor.[22-24] Typical inorganic semiconductors with indirect band gap show the best thermoelectric performance when the band gap is nk_BT, where n=6-10, k_B is the Boltzmann constant and T is the operating temperature of the device. On the other hand, semiconductors with direct band gap show that the optimum gap is always greater than $6k_BT$ (0.16 eV band gap calculated from $6k_BT$ at 298 K). It has been experimentally reported that few layered reduced GO has the band gap from 2.8 to 0.02 eV depending on the amount of oxygen containing functional groups.[25,26] In addition, previous theoretical studies have suggested that the band gap of graphene changes form direct to indirect with increasing oxidation level, due to the change of the highest valence band state from the bonding π orbital to the O 2p orbital.[27,28] Therefore, finding the optimum band gap of graphene is necessary to get the best thermoelectric performance. Although this study shows a quite low ZT value, it could be meaningful to report the experimental evidence that ZT of graphene derivatives can be controlled by oxidation level of graphene. Further investigation into thermoelectric properties of graphene and its derivatives depending on the band gap and doping of graphene has been in progress.

Conclusions

In summary, the chemical reduction of GO to rGO with hydrazine was controlled by differing the amount of hydrazine.

After purification and drying, rGOs were quantitatively and qualitatively characterized by XPS. XPS results demonstrate that the O/C area ratio of rGO decreases as the amount of hydrazine increases, thereby resulting in the control of the oxidation level of rGO. This study also demonstrates that the electrical conductivity of rGO can be improved with lower oxidation level of rGO. However, the increasing the electrical conductivity results in a decrease in the Seebeck coefficient. The thermal conductivity of rGO film with the oxidation level ($A_{O(1s)}/A_{C(1s)}$) of 0.32 was measured to 0.30 W/mK, which is 4 orders of magnitude lower than that of single-layer graphene (~5300 W/mK) due to the phonon scattering at the junctions of rGO nanoplatelets. The maximum ZT value was calculated to 1.1×10^{-4} from thermal conductivity of 0.30 W/mK and power factor ($S^2\sigma$) of 1.1×10^{-7} W/mK^2 for rGO sample with the oxidation level of 0.32.

References

(1) J. R. Sootsman, D. Y. Chung, and M. G. Kanatzidis, *Angew. Chem. Int. Ed. Engl.*, **48**, 8616 (2009).

(2) A. Majumdar, *Science,* **303**, 777 (2004).

(3) S. K. Bux, J. P. Fleurial, and R. B. Kaner, *Chem. Commun.,* **46**, 8311 (2010).

(4) E. J. Winder, A. B. Ellis, and G. C. Lisensky, *J. Chem. Educ.*, **73**, 940 (1996).

(5) Y. Ouyang and J. Guo, *Appl. Phys. Lett.*, **94**, 263107 (2009).

(6) L. Hao and T. K. Lee, *Phys. Rev. B*, **81**, 165445 (2010).

(7) N. Xiao, X. Dong, L. Song, D. Liu, Y. Tay, S, Wu, L.-J. Li, Y. Zhao, T. Yu, H. Zhang, W. Huang, H. H. Hng, P. M. Ajayan, and Q. Yan, *ACS Nano*, **5**, 2749 (2011).

(8) J. H. Seol, I. Jo, A. L. Moore, L. Lindsay, Z. H. Aitken, M. T. Pettes, X. Li, Z. Yao, R. Huang, D. Broido, N. Mingo, R. S. Ruoff, and L. Shi, *Science*, **328**, 213 (2010).

(9) N. I. Kovtyukhova, P. J. Ollivier, B. R. Martin, T. E. Mallouk, S. A. Chizhik, E. V. Buzaneva, and A. D. Gorchinskiy, *Chem. Mater.*, **11**, 771 (1999).

(10) W. S. Hummers and R. E. Offeman, *J. Am. Chem. Soc.*, **80**, 1339 (1958).

(11) D. Yang, A. Velamakanni, G. Bozoklu, S. Park, M. Stoller, R. D. Piner, S. Stankovich, I. Jung, D. A. Field, C. A. Ventride Jr., and R. S. Ruoff, *Carbon*, **47**, 145 (2009).

(12) S. Stankovich, D. A. Dikin, R. D. piner, K. A. Kohlhaas, A. Kleinhammes, Y. Jia, Y. Wu, S. T. Nguyen, and R. S. Ruoff, *Carbon*, **45**, 1558 (2007).

(13) A. Bagri, C. Mattevi, M. Acik, Y. J. Chabal, M. Chhowalla, and V. B. Shenoy, *Nat. Chem.*, **2**, 581 (2010).

(14) G. J. Snyder and E. S. Toberer, *Nat. Mater.*, **7**, 105 (2008).

(15) N. Dubey and M. Leclerc, *Polym. Phys.*, **49**, 467 (2009).

(16) Y. W. Park, Y. S. Lee, C. Park, L. W. Shacklette, and R. H. Baughman, *Solid State Commun.*, **63**, 1063 (1987).

(17) Y. Shinohara, K. Ohara, H. Nakanishi, Y. Imai, and Y. Isoda, *Mater. Sci. Forum*, **492-493**, 141 (2005).

(18) J. Li, X. Tang, H. Li, Y. Yan, and Q. Zhang, *Synth. Met.*, **160**, 1153 (2010).

(19) Y. Hiroshige, M. Ookawa, and N. Toshima, *Synth. Met.*, **157**, 467 (2007).

(20) E. Hu, A. Kaynak, and Y. Li, *Synth. Met.*, **150**, 139 (2005).

(21) A. A. Balandin, S. Ghosh, W. Bao, I. Calizo, D. Teweldebrhan, F. Miao, and C. N. Lau. *Nano Lett.*, **8**, 902 (2008).

(22) R. Chasmar and R. Stratton, *J. Electron. Control*, **7**, 52 (1959).

(23) G. D. Mahan, *J. Appl. Phys.*, **65**, 1578 (1989).

(24) J. O. Sofo and G. D. Mahan, *Phys. Rev. B*, **49**, 4565 (1994).

(25) Y. Shen, P. Zhou, Q. Q. Sun, L. Wan, J. Li, L. Y. Chen, D. W. Zhang, and X. B. Wang, *Appl. Phys. Lett.*, **99**, 141911 (2011).

(26) A. Mathkar, D. Tozier, P. Cox, P. Ong, C. Galande, K. Balakrishnan, A. Leela, M. Reddy, and P. M. Ajayan, *J. Phys. Chem. Lett.*, **3**, 986 (2012).

(27) T.-F. Yeh, J.-M. Syu, C. Cheng, T.-H. Chang, and H. Teng, *Adv. Funct. Mater.*, **20**, 2255 (2010).

(28) J. Ito, J. Nakamura, and A. Natori, *J. Appl. Phys.*, **103**, 113712 (2008).